AIAA JOURNAL
Vol. 30, No. 2, February 1992

Elastic-Plastic Finite Element Analysis of Thermoplastic Composite Plates and Shells

C. T. Sun* and G. Chen†
Purdue University, West Lafayette, Indiana 47907

A quadrilateral Mindlin-type plate finite element is developed for the elastic-plastic analysis of laminated composite plates and shells. A simple one-parameter plasticity model is used for characterizing the plastic behavior of the AS4/PEEK thermoplastic composite. A facet representation of the general shell geometry is adopted for the shell structural analysis. Numerical examples illustrate the effect of plasticity on the residual stresses in AS4/PEEK thermoplastic composite plates and shells after they are subjected to lateral pressures.

Introduction

UNLIKE thermosetting composites, advanced thermoplastic composites can be used to form structures by using conventional high-speed, hot-forming techniques and can be reformed under certain pressure and at certain temperature without losing their integrity and strength. However, understanding their forming behavior presents a challenge to manufacturing engineers. In forming fiber reinforced thermoplastic composites, conventional trial and error method may prove costly or even futile because of the many parameters that may affect the quality of the final product. High-speed computers combined with finite element technique provide us with powerful tools in simulating the forming process and optimizing various parameters, thereby saving much time and expense during the design stage.

The forming process of laminated thermoplastic composites often involves plastic bending deformations. Thus, an understanding of the elastic-plastic response of laminated thermoplastic composite plates and shells is very important.

Although considerable progress has been made in the elastic-plastic analysis of isotropic plate/shell structures, work on laminated composite plate/shell structures is limited. Whang[1] considered the elastoplastic finite element analysis of small deformation orthotropic plates and shells with strain hardening parameters. Owen and Figueiras[2,3] used the semiloof element and thick shell element to study the problem. Their nonlinear material models were based on Hill's modified von Mises yield function and the associated flow rule.[4-7]

In the present study, the four-noded Mindlin-type T-element[8,9] is chosen for its good performance in overcoming the "locking" difficulty without introducing the reduced integration technique, allowing the inclusion of bending-transverse shear coupling in plastic deformation. The one-parameter plastic constitutive model developed by Sun and Chen[10] is used because of its simplicity, which is even more attractive when cost becomes the overriding consideration in the nonlinear analysis. The facet approximation of general shell geometry[11,12] is adopted. The temperature-dependent material properties of AS4/PEEK advanced thermoplastic composites[13] are used in the numerical examples.

Received Oct. 15, 1990; revision received May 23, 1991; accepted for publication June 21, 1991.

*Professor, School of Aeronautics and Astronautics. Associate Fellow AIAA.

†Former Graduate Student, School of Aeronautics and Astronautics; currently, Product Engineer, Valeo Engine Cooling, Inc., Rochester, MI 48309.

Material Nonlinearity

A general yield function that is quadratic in stresses and includes transverse shear stress components is introduced:

$$2f(\{\sigma\}) - k = a_{11}\sigma_{11}^2 + a_{22}\sigma_{22}^2 + a_{33}\sigma_{33}^2 + 2a_{12}\sigma_{11}\sigma_{22} + 2a_{13}\sigma_{11}\sigma_{33} + 2a_{23}\sigma_{22}\sigma_{33} + 2a_{44}\sigma_{23}^2 + 2a_{55}\sigma_{31}^2 + 2a_{66}\sigma_{12}^2 - k = 0 \quad (1)$$

where σ_{ij} are stress components referring to the material principal axes (x_1, x_2, x_3), a_{ij} are coefficients bearing the orthotropic properties of the material, and k is a state variable depending on the plastic strain.

Using the associated flow rule, incremental plastic strains can be written in terms of the plastic potential as

$$\{d\varepsilon^p\} = d\lambda \frac{\partial f}{\partial \{\sigma\}} \quad (2)$$

where $\{d\varepsilon^p\}$ is the vector of plastic strain increments and $d\lambda$ is a proportionality factor.

For most advanced composites, plasticity in the fiber direction is negligible, i.e.,

$$d\varepsilon_{11}^p = 0 \quad (3)$$

which leads to the condition,

$$a_{11} = a_{12} = a_{13} = 0 \quad (4)$$

For thin and moderately thick plates, it is assumed that $\sigma_{33} = 0$. In general, $a_{55} = a_{66} \neq a_{44}$ for fiber composites. In Ref. 13, the value of a_{66} was determined experimentally. In this study, it is assumed that

$$a_{44} = a_{55} = a_{66} \quad (5)$$

Considering the above stated conditions and, without loss of generality, letting $a_{22} = 1$, the plastic potential function reduces to the one-parameter form:

$$2f = \sigma_{22}^2 + 2a_{66}(\sigma_{23}^2 + \sigma_{31}^2 + \sigma_{12}^2) \quad (6)$$

With Eq. (2), the increment of plastic work per unit volume can be written as

$$dW^p = \{\sigma\}^T\{d\varepsilon^p\} = 2f d\lambda \quad (7)$$

Define the effective stress $\bar{\sigma}$ as

$$\bar{\sigma} = \sqrt{3f} \quad (8)$$

Let the effective plastic strain increments $d\bar{\varepsilon}^p$ be defined as

$$dW^p = \bar{\sigma} d\bar{\varepsilon}^p \tag{9}$$

After some manipulations with the relations in Eqs. (2) and (7–9), the effective plastic strain increment $d\bar{\varepsilon}^p$ is obtained as

$$d\bar{\varepsilon}^p = \sqrt{\frac{2}{3}}\left\{(d\varepsilon_{22}^{p2})^2 + \frac{1}{2a_{66}}[(d\gamma_{12}^p)^2 + (d\gamma_{23}^p)^2 + (d\gamma_{31}^p)^2]\right\}^{1/2} \tag{10}$$

Assume that the incremental strain ($d\varepsilon$) is small, and can be decomposed linearly into the elastic part ($d\varepsilon^e$) and the plastic part ($d\varepsilon^p$), i.e.,

$$\{d\varepsilon\} = \{d\varepsilon^e\} + \{d\varepsilon^p\} \tag{11}$$

where

$$\{\varepsilon\}^T = \{\varepsilon_{11}, \varepsilon_{22}, \gamma_{12}, \gamma_{23}, \gamma_{31}\} \tag{12}$$

The incremental stress-strain relation for the elastic part is

$$\{d\sigma\} = [Q^e](\{d\varepsilon\} - \{d\varepsilon^p\}) \tag{13}$$

in which $[Q^e]$ is the elastic stiffness matrix given by

$$[Q^e] = [S^e]^{-1} \tag{14}$$

where the elastic compliance matrix is

$$(S^e) = \begin{bmatrix} \frac{1}{E_1} & -\frac{\nu_{12}}{E_1} & 0 & 0 & 0 \\ -\frac{\nu_{12}}{E_1} & \frac{1}{E_2} & 0 & 0 & 0 \\ 0 & 0 & \frac{1}{G_{12}} & 0 & 0 \\ 0 & 0 & 0 & \frac{1}{G_{23}} & 0 \\ 0 & 0 & 0 & 0 & \frac{1}{G_{31}} \end{bmatrix} \tag{15}$$

In Eq. (15), E_1 and E_2 are the longitudinal and transverse elastic moduli, respectively, ν_{12} is the Poisson's ratio measuring contraction in the x_2-direction when loading is in the x_1-direction, and G_{ij} are the shear moduli.

In order to derive the elastic-plastic constitutive matrices, we start from the consistency condition, i.e., during plastic deformation, stresses remain on the yield surface so that

$$\left(\frac{\partial f}{\partial\{\sigma\}}\right)^T \{d\sigma\} - \frac{1}{2}\frac{dk}{d\bar{\varepsilon}^p} d\bar{\varepsilon}^p = 0 \tag{16}$$

From Eqs. (2), (6), (13), and (16) and defining plastic modulus H as $H = d\bar{\sigma}/d\bar{\varepsilon}^p$, we derive the relation between the plastic strain increment and the total strain increment as

$$\{d\varepsilon^p\} = d\lambda \frac{\partial f}{\partial\{\sigma\}} = \frac{\partial f}{\partial\{\sigma\}} \frac{\left(\frac{\partial f}{\partial\{\sigma\}}\right)^T [Q^e]\{d\varepsilon\}}{\frac{4}{9}\bar{\sigma}^2 H + \left(\frac{\partial f}{\partial\{\sigma\}}\right)^T [Q^e]\frac{\partial f}{\partial\{\sigma\}}} \tag{17}$$

Finally, from Eqs. (13) and (17) the relation between the stress increment $\{d\sigma\}$ and the total strain increment $\{d\varepsilon\}$ is obtained. We have

$$\{d\sigma\} = [Q^{ep}]\{d\varepsilon\} \tag{18}$$

in which the elastic-plastic stiffness matrix is defined as

$$[Q^{ep}] = [Q^e] - [Q^e]\frac{\frac{\partial f}{\partial\{\sigma\}}\left(\frac{\partial f}{\partial\{\sigma\}}\right)^T [Q^e]}{\frac{4}{9}\bar{\sigma}^2 H + \left(\frac{\partial f}{\partial\{\sigma\}}\right)^T [Q^e]\frac{\partial f}{\partial\{\sigma\}}} \tag{19}$$

Thus, in the elastic-plastic analysis, the plastic modulus H must be given at all stress levels. The hardening law for AS4/PEEK composite can be modeled by a simple power law as[13]

$$\bar{\varepsilon}^p = \alpha(\bar{\sigma})^\beta \tag{20}$$

In addition, the value of a_{66} in the plastic potential function must be determined.

Mindlin Plate Finite Element

The Mindlin plate theory is employed to model the elastic-plastic deformation of the composite laminate. The transverse shear deformation is thus accounted for. The plate displacement field is approximated by

$$\begin{aligned} u &= u_0(x, y) - z\Psi_x(x, y) \\ v &= v_0(x, y) - z\Psi_y(x, y) \\ w &= w_0(x, y) \end{aligned} \tag{21}$$

where u_0, v_0, and w_0 are the midplane displacement components in the x-, y-, and z-directions, respectively; Ψ_x and Ψ_y are the rotation of the cross sections about the y- and x-axis, respectively, see Fig. 1. The corresponding strain components are

$$\{\tilde{\varepsilon}\} = \begin{Bmatrix} \tilde{\varepsilon}^0 \\ 0 \end{Bmatrix} + \begin{Bmatrix} z\tilde{\kappa} \\ \tilde{\gamma}_z^0 \end{Bmatrix} \tag{22}$$

where the tilde refers to the geometric coordinate system (x, y, z) as shown in Fig. 1, and

$$\{\tilde{\varepsilon}^0\}^T = \{\varepsilon_{xx}^0, \varepsilon_{yy}^0, \gamma_{xy}^0\} \tag{23}$$

$$\{\tilde{\kappa}\}^T = \{\kappa_{xx}, \kappa_{yy}, \kappa_{xy}\} \tag{24}$$

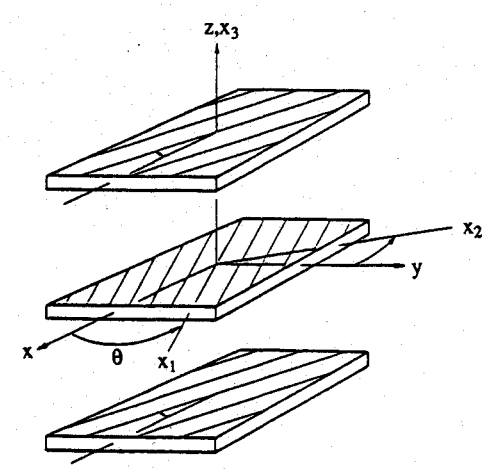

Fig. 1 Reference coordinates for laminates.

$$\{\tilde{\gamma}_z^0\}^T = \{\gamma_{yz}^0,\ \gamma_{zx}^0\} \tag{25}$$

are in-plane strains, curvatures, and transverse shear strains, respectively. In terms of the plate kinematic variables, we have

$$\{\tilde{\varepsilon}^0\} = \begin{Bmatrix} \dfrac{\partial u_0}{\partial x} \\ \dfrac{\partial v_0}{\partial y} \\ \dfrac{\partial u_0}{\partial y} + \dfrac{\partial v_0}{\partial x} \end{Bmatrix} \tag{26}$$

$$\{\tilde{\kappa}\} = \begin{Bmatrix} -\dfrac{\partial \Psi_x}{\partial x} \\ \dfrac{\partial \Psi_y}{\partial y} \\ -\dfrac{\partial \Psi_x}{\partial y} - \dfrac{\partial \Psi_y}{\partial x} \end{Bmatrix} \tag{27}$$

$$\{\tilde{\gamma}_z^0\} = \begin{Bmatrix} \dfrac{\partial w}{\partial y} - \Psi_y \\ \dfrac{\partial w}{\partial x} - \Psi_x \end{Bmatrix} \tag{28}$$

Consider a typical layer in the laminate. The incremental elastic-plastic stress-strain relations are given by

$$\{d\tilde{\sigma}\} = [\overline{Q}^{ep}]\ \{d\tilde{\varepsilon}\} \tag{29}$$

in which $[\overline{Q}^{ep}]$ is the elastic-plastic stiffness matrix referring to the xyz coordinate system. It should be noted that $[\overline{Q}^{ep}]$ is fully populated and will cause in-plane and bending deformations to couple with transverse shear deformation during the plastic deformation stage.

Integrations of incremental stresses and multiplications of incremental stresses with z over the thickness of the laminates h yield the incremental in-plane resultant forces, moments, and transverse shear forces as

$$\{dN\} = \begin{Bmatrix} dN_{xx} \\ dN_{yy} \\ dN_{xy} \end{Bmatrix} = \int_{-h/2}^{h/2} \begin{Bmatrix} d\sigma_{xx} \\ d\sigma_{yy} \\ d\sigma_{xy} \end{Bmatrix} dz$$

$$= [A]\ \{d\tilde{\varepsilon}^0\} + [B]\ \{d\tilde{\kappa}\} + [E]\ \{d\tilde{\gamma}_z\} \tag{30}$$

$$\{dM\} = \begin{Bmatrix} dM_{xx} \\ dM_{yy} \\ dM_{xy} \end{Bmatrix} = \int_{-h/2}^{h/2} \begin{Bmatrix} d\sigma_{xx} \\ d\sigma_{yy} \\ d\sigma_{xy} \end{Bmatrix} z\ dz$$

$$= [B]\ \{d\tilde{\varepsilon}^0\} + [D]\ \{d\tilde{\kappa}\} + [F]\ \{d\tilde{\gamma}_z^0\} \tag{31}$$

$$\{dQ\} = \begin{Bmatrix} dQ_{yz} \\ dQ_{zx} \end{Bmatrix} = \int_{-h/2}^{h/2} \begin{Bmatrix} d\sigma_{yz} \\ d\sigma_{xz} \end{Bmatrix} dz$$

$$= [E]^T\{d\tilde{\varepsilon}^0\} + [F]^T\{d\tilde{\kappa}\} + [H]\{d\tilde{\gamma}_z^0\} \tag{32}$$

To facilitate the integrations of the stiffness matrices $[A]$, $[B]$, $[E]$, etc., a numerical scheme is used. We first divide each lamina into several layers for integration. This would result in a total of n layers for the laminate. Along the thickness-direction (z-axis), stress is assumed to be uniform over the thickness in each layer, and its value is taken to be equal to that at the midplane of that layer. Thus, the stress distribution over the thickness of the laminate is a piecewise constant approximation, see Fig. 2. As a result, the elements in the stiffness matrices in Eqs. (30–32) are given by:

$$A_{ij} = \sum_{k=1}^{n} \overline{Q}_{ij}^{ep}(z_{k+1} - z_k), \qquad i, j = 1, 2, 6 \tag{33}$$

$$B_{ij} = \sum_{k=1}^{n} \frac{1}{2} \overline{Q}_{ij}^{ep}(z_{k+1}^2 - z_k^2), \qquad i, j = 1, 2, 6 \tag{34}$$

$$D_{ij} = \sum_{k=1}^{n} \frac{1}{4} \overline{Q}_{ij}^{ep}(z_{k+1} + z_k) \times (z_{k+1}^2 - z_k^2), \qquad i, j = 1, 2, 6 \tag{35}$$

$$E_{ij} = \sum_{k=1}^{n} \overline{Q}_{ij}^{ep}(z_{k+1} - z_k), \qquad i = 1, 3;\ j = 4, 5 \tag{36}$$

$$F_{ij} = \sum_{k=1}^{n} \frac{1}{2} \overline{Q}_{ij}^{ep}(z_{k+1}^2 - z_k^2), \qquad i = 1, 3;\ j = 4, 5 \tag{37}$$

$$H_{ij} = \sum_{k=1}^{n} \overline{Q}_{ij}^{ep}(z_{k+1} - z_k), \qquad i, j, = 4, 5 \tag{38}$$

The finite element formulation proposed by Hughes and Tezduyar[8] is employed in this study to develop an isoparametric four-noded plate element according to Mindlin plate theory. The essence in this formulation lies in the fact that the bilinear interpolation in the element is imposed on transverse strain components rather than on displacements. First, the transverse shear strains at a node of an element are obtained by interpolating the transverse shear strains at the respective midpoints of the two edges meeting at that node and taking the average values. These average nodal values are then used in conjunction with the same shape functions to interpolate the transverse shear strains in the entire element. This formulation is capable of relieving the shear locking problem often encountered in using Mindlin plate finite element to solve thin plate problems.

Analysis of Shells

In this study, a shell is replaced by an assembly of flat finite elements of quadrilateral shape. The stiffness properties of

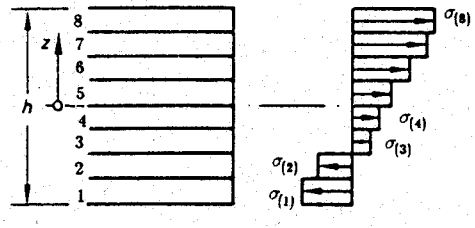

Fig. 2 Stress profile of layered model.

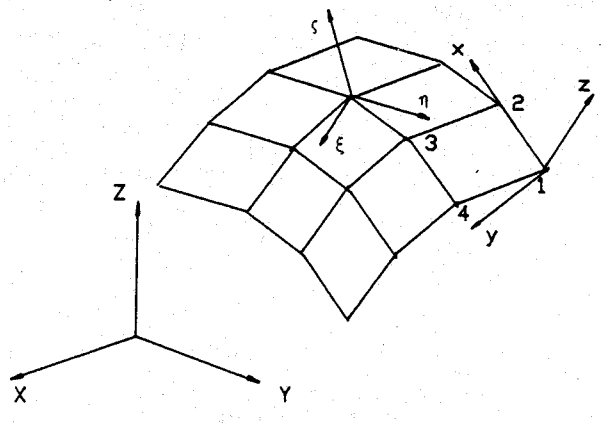

Fig. 3 Coordinate systems for shell analysis.

an individual element are defined in a local Cartesian element coordinate system (x, y, z) specified for that particular element (Fig. 3). This is a moving reference frame that translates and rotates with the element. Shown in Fig. 3 is a fixed global coordinate system (X, Y, Z) used to define the location of the nodal points. At each node a moving surface Cartesian coordinate system (ξ, η, ζ) is introduced. The surface coordinate system is defined in such a way that the ζ-direction is always taken normal to the current shell surface at the particular nodal point; hence, the ξ- and η-axes lie in the tangent plane. The common reference frame to which all element properties are transformed prior to the assembly of stiffnesses are the *base coordinates*. The base coordinates are composed of a special combination of global coordinates and surface coordinates.

The relation between global and element coordinates is given by a standard coordinate transformation defined by the matrix of direction cosines of the element coordinate systems $[G]$:

$$\begin{Bmatrix} X \\ Y \\ Z \end{Bmatrix} = [G] \begin{Bmatrix} x \\ y \\ z \end{Bmatrix} \tag{39}$$

where $[G]$ is the matrix of the direction cosines of the element coordinates:

$$[G] = \begin{bmatrix} \cos(X, x) & \cos(X, y) & \cos(X, z) \\ \cos(Y, x) & \cos(Y, y) & \cos(Y, z) \\ \cos(Z, x) & \cos(Z, y) & \cos(Z, z) \end{bmatrix} \tag{40}$$

The relation between global and surface coordinates can be expressed as

$$\begin{Bmatrix} X \\ Y \\ Z \end{Bmatrix} = [S] \begin{Bmatrix} \xi \\ \eta \\ \zeta \end{Bmatrix} \tag{41}$$

where $[S]$ is the matrix of direction cosines of the surface coordinate system

$$[S] = \begin{bmatrix} \cos(X, \xi) & \cos(X, \eta) & \cos(X, \zeta) \\ \cos(Y, \xi) & \cos(Y, \eta) & \cos(Y, \zeta) \\ \cos(Z, \xi) & \cos(Z, \eta) & \cos(Z, \zeta) \end{bmatrix} \tag{42}$$

From Eqs. (39) and (41), it then follows that

$$\begin{Bmatrix} \xi \\ \eta \\ \zeta \end{Bmatrix} = [S]^T[G] \begin{Bmatrix} x \\ y \\ z \end{Bmatrix} = [C] \begin{Bmatrix} x \\ y \\ z \end{Bmatrix} \tag{43}$$

The Mindlin type T-element employed here has five degrees of freedom at each of the four corner nodes with respect to the element coordinate system, i.e., the translations (u_0, v_0, w_0) in the x- , y- , and z-directions and the rotations (Ψ_x, Ψ_y) about the y- and x-axis, respectively. The global coordinates are taken as base coordinates for the translation degrees of freedom (u_B, v_B, w_B), whereas surface coordinates are used for rotations (Ψ_ξ, Ψ_η). Only two rotations among the nodal degrees of freedom with the third component about the surface normal being neglected, the singularity that occurs when elements around a node are almost coplanar can be avoided.

The transformations of displacement components between the element coordinates and the base coordinates for node i are given by

$$\{U_B\}_i^e = \begin{bmatrix} (G) & 0 \\ 0 & (I)_e(b)_i(I)_e^T \end{bmatrix} \begin{bmatrix} u_0 \\ v_0 \\ w_0 \\ \Psi_x \\ \Psi_y \end{bmatrix}_i = (T)_i(U)_i^e \tag{44}$$

where

$$[I]_e = \begin{bmatrix} 0 & 1 \\ -1 & 0 \end{bmatrix} \tag{45}$$

$$\{U_B\}_i^e = \begin{Bmatrix} u_B \\ v_B \\ w_B \\ \Psi_\xi \\ \Psi_\eta \end{Bmatrix}_i \tag{46}$$

and $[b]_i$ is the upper left 2×2 submatrix of $[C]$ in Eq. (43) for local nodal point number i $(i = 1, 2, 3, 4)$; $[I]_e$ results from the definition of sign convention of rotation degrees of freedom in element coordinates and base coordinates. The subscript B has been introduced to identify a quantity that refers to the base coordinates. However, one should note that in $\{U_B\}$, the rotations of Ψ_ξ and Ψ_η refer to the surface coordinates.

For the entire element displacement vector, it then follows that

$$\{U_B\}^e = [T]\{U\}^e \tag{47}$$

where

$$[T] = \begin{bmatrix} [T]_1 & 0 & 0 & 0 \\ 0 & [T]_2 & 0 & 0 \\ 0 & 0 & [T]_3 & 0 \\ 0 & 0 & 0 & [T]_4 \end{bmatrix} \tag{48}$$

Using the above transformation relations, the external load vector and the stiffness matrix of an element in the base coordinate system are obtained by the transformations

$$\{R_B\}^e = [T]\{R\}^e \tag{49}$$

and

$$[K_B]^e = [T][K]^e[T]^T \tag{50}$$

Numerical Procedure and Results

Because of the nonlinear elastic-plastic stress-strain relations, the assembled system of equations for the finite element system is also nonlinear. An incremental load procedure in conjunction with the standard Newton-Raphson technique is employed for solving the nonlinear systems of equations. The material stiffness (constitutive) matrices are evaluated at each Gaussian point, in each layer, in each lamina and in each element during every iteration. For an equilibrium iteration, convergence is achieved when the out-of-balance forces, i.e., the difference between the internal force and the external force, becomes less than a prescribed tolerance in a Euclidean norm sense. Additional details of the computational procedure can be found in Ref. 14.

Several numerical examples are studied to illustrate the capabilities of the proposed computational procedure. The composite material considered in the examples is AS4/PEEK thermoplastic composite whose elastic and plastic properties at room temperature are[13]

$$E_1 = 18.5 \times 10^6 \text{ psi}, \quad E_2 = 1.49 \times 10^6 \text{ psi}$$

$$G_{12} = 0.99 \times 10^6 \text{ psi}, \quad \nu_{12} = 0.28$$

$$a_{66} = 1.5, \quad \beta = 7.0, \quad \alpha = 2.07 \times 10^{-10} \tag{51}$$

In addition, the following assumptions are adopted:

$$\nu_{23} = \nu_{13} = \nu_{12}, \quad G_{23} = G_{31} = G_{12} \tag{52}$$

It should be noted that when the values of α and β given by Eq. (51) are used, the unit of the effective stress in Eq. (20) must be *ksi*. Adjustment of these values must be made if different units for stress are used.

All computations are performed on the VAX/780 computer with double precision.

Clamped Isotropic Plate

A square plate (10 m × 10 m × 0.1 m) clamped along the edges is analyzed using both the present finite element and the general purpose finite element package MARC. One quadrant of the plate is discretized by 4 elements, and 10 equal layers are taken through the thickness. Eight load steps are used.

The material is assumed to be isotropic and elastic-plastic with a linear hardening behavior. The elastic constants are given by

$$E = 10.9 \times 10^5 \text{ N/m}^2, \qquad \nu = 0.3 \tag{53}$$

The yield stress is

$$\sigma_y = 1230 \text{ N/m}^2 \tag{54}$$

and the plastic modulus is

$$H = \frac{d\bar{\sigma}}{d\bar{\varepsilon}^p} = 5000 \tag{55}$$

Figure 4 presents the vertical displacements as the central point at different load levels. It is evident that the two solutions agree very well.

Clamped Laminated Composite Plates

Rectangular laminated plates of AS4/PEEK thermoplastic composite under a uniformly distributed pressure are considered. The plate is clamped all around. Plate dimensions are shown in Fig. 5.

Both $[0_2/45_2/-45_2/90_2]_s$ and $[90_2/45_2/-45_2/0_2]_s$ laminates are studied. Each ply is assumed to be 0.005 in. Thus, the total plate thickness is 0.08 in. The entire plate is discretized with 8 × 4 elements and 16 equal layers through the plate thickness.

Figure 6 presents the load vs central deflection curves for both laminated plates. It is evident that stacking sequence plays a very important role in the stiffness and plastic responses of the laminate.

Figures 7 and 8 show the residual stress profiles from the top surface to the midplane at the central point of the $[0_2/45_2/-45_2/90_2]_s$ and $[0_2/45_2/-45_2/0_2]_s$ laminated plates, respectively. Again, the state of residual stresses in the laminate is highly dependent on the stacking sequence.

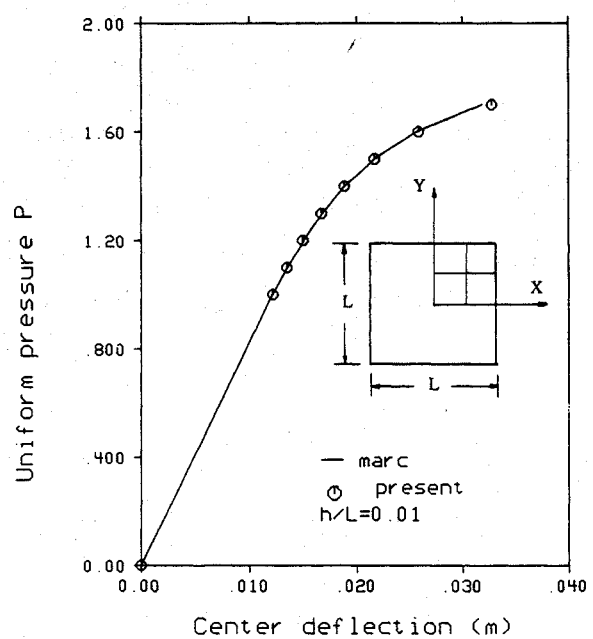

Fig. 4 Central deflection for isotropic plate subjected to uniform lateral pressure P (N/m²).

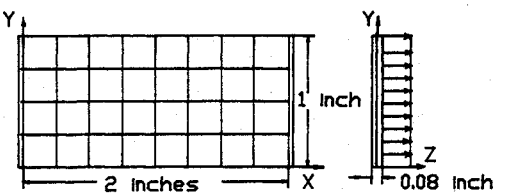

Fig. 5 Geometry of laminated thermoplastic composite plate subjected to uniform lateral pressure.

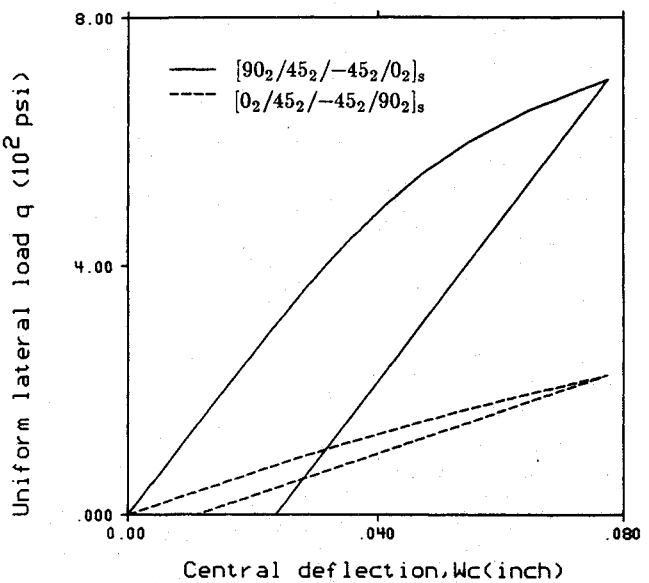

Fig. 6 Central deflections for $[0_2/45_2/-45_2/90_2]_s$ and $[90_2/45_2/-45_2/0_2]_s$ laminated thermoplastic composite plates subjected to uniform lateral pressure.

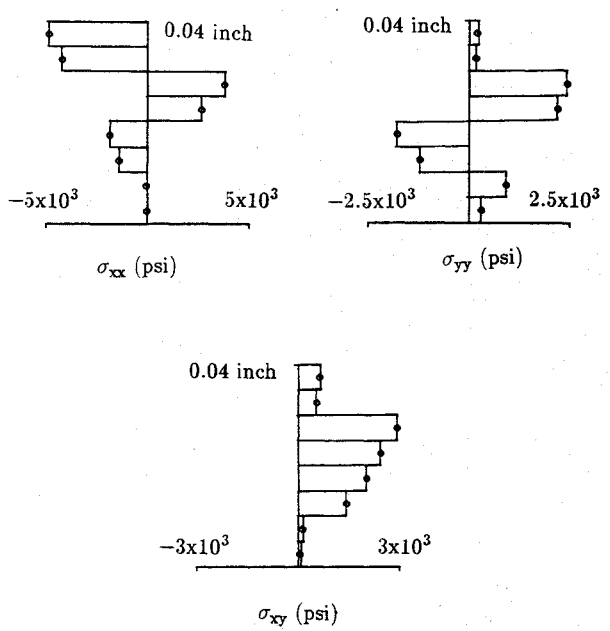

Fig. 7 Central residual stresses along thickness for the $[0_2/45_2/-45_2/90_2]_s$ laminated thermoplastic composite plate after unloading.

Laminated Composite Shells

A cylindrical shell under a uniformly distributed pressure as shown in Fig. 9 is considered. The two longitudinal edges are clamped while the curved edges are free. A quadrant of the shell is modeled by 6 × 8 elements (see Fig. 9), and 16 equal layers are taken through the thickness.

Two AS4/PEEK laminates are considered; i.e., $[0_4/90_4]_s$ and $[90_4/0_4]_s$. The elastic plastic properties are given by Eq. (51). The load-deflection curves at the central point for both laminates are linear and almost identical indicating that these two laminates have almost the same stiffness. This is because the two laminates have the same membrane stiffness, and, in this cylindrical shell, the membrane stiffness dominates deflection.

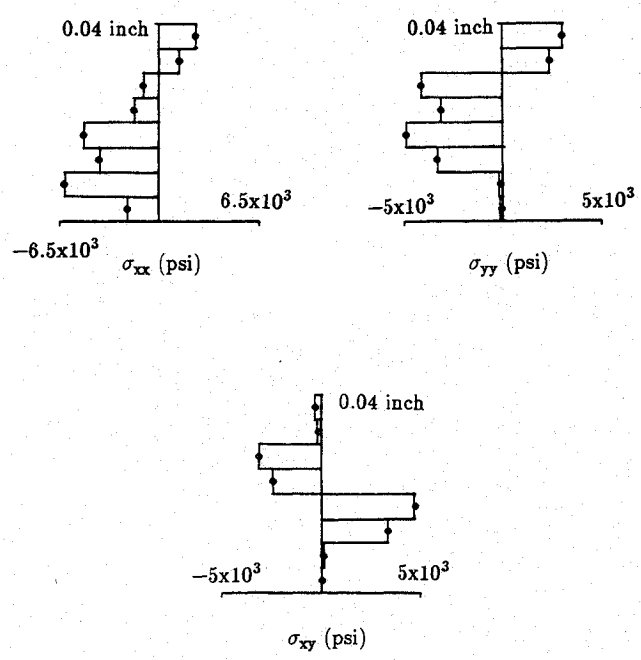

Fig. 8 Central residual stresses along thickness for the $[90_2/45_2/-45_2/0_2]_s$ laminated thermoplastic composite plate after unloading.

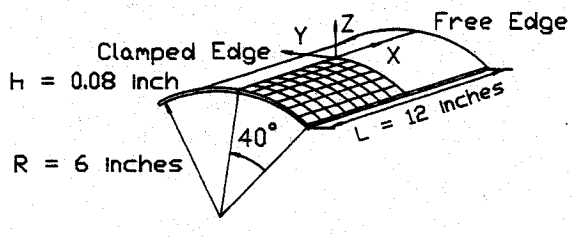

Fig. 9 Geometry of laminated thermoplastic composite shell subjected to uniform lateral pressure.

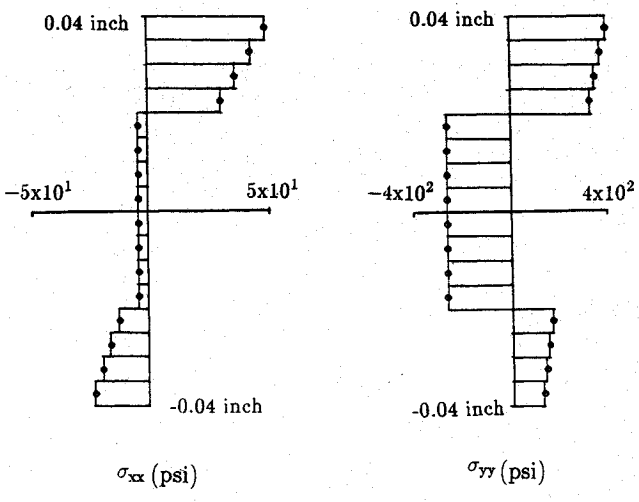

Fig. 10 Central residual stresses along thickness for the $[0_4/90_4]_s$ laminated thermoplastic composite shell after unloading from a peak load of $q = -700$ psi.

Figure 10 shows the residual stresses over the thickness at the central point of the $[0_4/90_4]_s$ shell after unloading from a peak load of $q = -700$ psi. It is interesting to note that the level of residual stress is quite high even though the load-deflection curve shows little nonlinear behavior. Also note that the transverse residual stresses σ_{yy} in the 0 deg—plies are all tensile.

Summary

A finite element code and the associated computational procedure were developed for the elastic-plastic analysis of laminated composite plates and shells. A one-parameter plasticity model was used to describe the orthotropic plasticity in the composite, and the Mindlin plate theory was used to formulate the plate finite element. A numerical example for an isotropic plate under lateral loading was solved by both the present finite element code and by the general purpose finite element package MARC. Good agreement of the two solutions was obtained. Other numerical examples show some interesting characteristics of elastic-plastic behavior in AS4/PEEK thermoplastic composite plates and shells.

Acknowledgment

This research was supported by the National Science Foundation under Grant CDR 880317 to the Engineering Research Center for Intelligent Manufacturing Systems at Purdue University.

References

[1]Whang, B., "Elasto-Plastic Orthotropic Plates and Shells," *Proceedings of the Symposium on Application of Finite Element Method in Civil Engineering*, Vanderbilt University, TN, 1969.

[2]Owen, D. R. J., and Figueiras, J. A., "Elasto-Plastic Analysis of Anisotropic Plates and Shells by the Semiloof Element," *International Journal for Numerical Methods in Engineering*, Vol. 19, No. 4, 1983, pp. 521–539.

[3]Owen, D. R. J., and Figueiras, J. A., "Anistropic Elasto-Plastic Finite Element Analysis of Thick and Thin Plates and Shells," *International Journal for Numerical Methods in Engineering*, Vol. 19, No. 4, 1983, pp. 551–566.

[4]Hill, R., "A Theory of Yielding and Plastic Flow of Anisotropic Metals," *Proceedings of the Royal Society of London*, London, England, UK, 1948, Ser. 123.

[5]Hu, L. W., "Studies on Plastic Flow of Anisotropic Metals," *Journal of Applied Mechanics*, Vol. 23, No. 3, 1956, pp. 444–450.

[6]Shih, C. F., and Lee, D., "Further Developments in Anisotropic Plasticity," *Journal of Engineering Materials and Technology*, Vol. 100, No. 3, 1978, p. 294–309.

[7]Valliappan, S., Boonlaulohr, P., and Lee, I. K., "Non-Linear Analysis for Anisotropic Materials," *International Journal for Numerical Methods in Engineering*, Vol. 10, No. 3, 1976, pp. 597–606.

[8]Hughes, T. J. R., and Tezduyar, T. E., "Finite Element Based Upon Mindlin Plate Theory With Particular Reference to the Four-Node Bilinear Isoparametric Element," *Journal of Applied Mechanics*, Vol. 48, No. 3, 1981, pp. 587–596.

[9]MacNeal, R. H., "Derivation of Element Stiffness Matrices by Assumed Strain Distributions," *Nuclear Engineering and Design*, Vol. 70, No. 1, 1982, pp. 3–12.

[10]Sun, C. T., and Chen, J. L., "A Simple Flow Rule for Characterizing Nonlinear Behavior of Fiber Composites," *Journal of Composite Materials*, Vol. 23, No. 10, 1989, pp. 1009–1020.

[11]Horrigmoe, G., and Bergan, P. G., "Nonlinear Analysis of Free-Form Shell by Flat Finite Elements," *Computer Methods in Applied Mechanics*, Vol. 16, No. 1, 1978, pp. 11–35.

[12]Horrigmoe, G., "Hybrid Stress Finite Element Model for Non-Linear Shell Problems," *International Journal for Numerical Methods in Engineering*, Vol. 12, No. 2, 1978, pp. 1819–1839.

[13]Sun, C. T., and Yoon, K. J., "Characterization of Elastic-Plastic Properties of AS4/APC-2 Thermoplastic Composite," to appear in *Journal of Composite Materials*.

[14]Chen, G., "Nonlinear Finite Element Analysis of Plates and Shells of Composite Laminates," Master's Thesis, School of Aeronautical and Astronautical Engineering, Purdue University, IN, 1988.